Quantum recurrences in the kicked top

Amit Anand [1,2,*] Jack Davis [1,2,3] and Shohini Ghose [1,4,5]

[1]*Institute for Quantum Computing, University of Waterloo, Waterloo, Ontario, Canada N2L 3G1*
[2]*Department of Physics and Astronomy, University of Waterloo, Waterloo, Ontario, Canada N2L 3G1*
[3]*DIENS, École Normale Supérieure, PSL University, CNRS, INRIA, 45 rue d'Ulm, Paris 75005, France*
[4]*Department of Physics and Computer Science, Wilfrid Laurier University, Waterloo, Ontario, Canada N2L 3C5*
[5]*Perimeter Institute for Theoretical Physics, 31 Caroline St N, Waterloo, Ontario, Canada N2L 2Y5*

(Received 20 November 2023; accepted 2 April 2024; published 3 May 2024)

The emergence of classical chaos from an underlying quantum mechanics remains a challenging question due to the differences between dynamics driven by Schrödinger's equation versus Newton's equations. We present an infinite family of purely quantum recurrences that are not present in the classical limit of a chaotic system. They take the form of stroboscopic unitary evolutions in the quantum kicked top that act as the identity after a finite number of kicks. These state-independent recurrences are present in all finite dimensions and depend on the strength of the chaoticity parameter of the top. We further discuss the relationship of these periodicities to the quantum kicked rotor dynamics and the phenomenon of quantum antiresonance.

DOI: 10.1103/PhysRevResearch.6.023120

I. INTRODUCTION

The quantum-classical correspondence principle broadly states, in its commonly understood form, that the predictions of a dynamically evolving quantum system should reproduce the predictions of a classical system under appropriate circumstances [1]. This sometimes takes the form of a particular limit of some set of parameters that characterize the quantum system (i.e., large quantum numbers, vanishing Planck action, etc.). In such situations the transition may be called a *classical limit* of the quantum system [2]. On the other hand, it is well known that classical systems can display chaotic behavior—broadly defined as high sensitivity to initial conditions. Interestingly, in quantum systems that have a chaotic classical limit, the quantum-to-classical transition is not as well understood [3–6]. Exploring such systems can thus provide insight into the differences between quantum and classical dynamics and the fundamental origin of chaotic phenomena.

A useful model studied in this context is the quantum kicked top [7]. This model is a spin-j system subject to a Floquet evolution (i.e., a stroboscopic dynamics). It is of interest because it lives in a finite-dimensional Hilbert space, its dynamics have a well-defined classical limit ($j \to \infty$) with an easily tunable degree of chaos via its Hamiltonian parameters, and it is experimentally feasible [8–10]. Furthermore, the alternative representation of any spin-j system as a many-body system of indistinguishable qubits has led to much work on understanding the surprisingly subtle relationship between dynamical entanglement, Hilbert space dimension, and emergent chaos in the kicked top model [6,11–16].

In this paper we probe the quantum versus classical dynamics in the kicked top and present a surprising result. For a given value of spin j, we can always find values of the chaoticity parameter κ that generate regular, periodic dynamics, independent of the initial state of the system. In contrast, the corresponding set of classical dynamics for the same κ values is chaotic. In particular, we analytically and numerically show that, in all Hilbert space dimensions, the kicked top displays several state-independent, temporal periodicities/recurrences: three for integer spin values and two for half-integer spin values. Whereas previous work has explored a specific temporal periodicity in a semiclassical limit [17], the general set of recurrences derived in our analysis have not been previously identified. Because these recurrences are state independent and generally occur at large chaoticity values, they have no classical analog. Note that the recurrence-inducing Hamiltonian parameters we identify are dimension dependent. That is, while chaos still emerges in the classical limit for any fixed chaoticity value, our results demonstrate that the transition to classical behavior does not smoothly vary with the size of the system. Our analysis also resolves previous conflicting results on how the chaoticity parameter κ in the kicked top influences the presence of quantum temporal periodicity [14]. In addition we establish a relationship between our kicked top periodicities and the quantum resonances identified in the kicked rotor. Our results highlight the complex nature of quantum chaos.

II. BACKGROUND

The quantum kicked top (QKT) is a finite-dimensional dynamical model used to study quantum chaos, known for

*a63anand@uwaterloo.ca

its compact phase space and parametrizable chaoticity structure [7]. The time-dependent, periodically driven system is governed by the Hamiltonian

$$H = \hbar\frac{pJ_y}{\tau} + \hbar\frac{\kappa J_z^2}{2j}\sum_{n=-\infty}^{\infty}\delta(t-n\tau), \tag{1}$$

where $\{J_x, J_y, J_z\}$ are the generators of angular momentum: $[J_i, J_k] = i\epsilon_{ikl}J_l$. It describes a spin of size j precessing about the y axis together with impulsive state-dependent twists about the z axis with magnitude characterized by the chaoticity parameter κ. The period between kicks is τ and p is the amount of y precession within one period. The associated Floquet time evolution operator for one period is

$$U_\kappa = \exp\Big(-i\frac{\kappa}{2j}J_z^2\Big)\exp\Big(-i\frac{p}{\tau}J_y\Big), \tag{2}$$

where κ indexes the chaoticity value of the dynamics.

The classical kicked top can be obtained by computing the Heisenberg equations for the rescaled angular momentum generators, $X_i = J_i/j$, satisfying $[X_i, X_k] = (1/j)\epsilon_{ikl}X_l$ and followed by the limit $j \to \infty$ [7]. In the commonly considered case of $(\tau = 1, p = \pi/2)$, the classical map is

$$\begin{aligned} X_{n+1} &= Z_n\cos(\kappa X_n) + Y_n\sin(\kappa X_n),\\ Y_{n+1} &= Y_n\cos(\kappa X_n) - Z_n\sin(\kappa X_n),\\ Z_{n+1} &= -X_n. \end{aligned} \tag{3}$$

As the chaoticity parameter κ is varied the classical dynamics ranges from completely regular motion ($\kappa \leqslant 2.1$) to a mixture of regular and chaotic motion ($2.1 \leqslant \kappa \leqslant 4.4$) to fully chaotic motion ($\kappa > 4.4$) [6]. The classical stroboscopic map in polar coordinates for a set of initial conditions with $\kappa = 2.5$ and $\kappa = 3.0$ is given in Fig. 1(a) and Fig. 1(b), respectively. When comparing the quantum and classical systems, a common approach is to quantify the difference between the quantum dynamics of a quantum state (usually spin coherent) with the classical dynamics of a classical state (usually a point or a distribution with the same centroid as the spin coherent state). Importantly, the Hamiltonian parameter κ appearing in Eqs. (2) and (3) is the same for both systems.

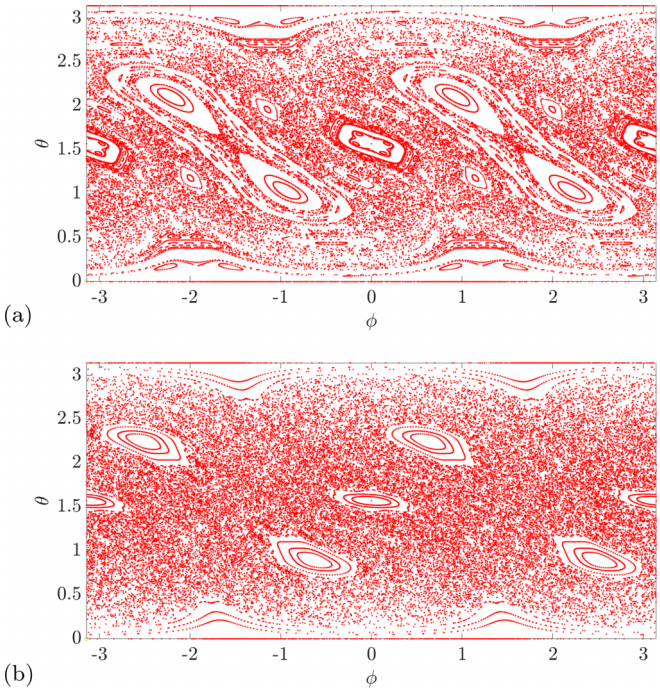

FIG. 1. Stroboscopic map showing the classical time evolution over 150 kicks for (a) $\kappa = 2.5$ and (b) $\kappa = 3.0$ for several hundred initial points.

III. PERIODICITY IN TWIST STRENGTH

We begin by first showing a relevant nontemporal periodicity in κ. As pointed out in [18], there is a recurrent relationship between unitaries U_κ (1) separated by an amount $\Delta\kappa = 2\pi j$: $U_{\kappa+2\pi j} = e^{-i\pi J_z^2}U_\kappa$. The unitary $e^{-i\pi J_z^2}$ characterizes the difference between the actions of U_κ and $U_{\kappa+2\pi j}$ in Hilbert space. We show that this operator acts as a symmetric local unitary in the qubit picture and so does not modify any correlations between qubits.

Denoting $Z_m := \sigma_z^{(m)}$ as the Pauli Z operator acting on the mth qubit (spin-1/2), we consider the operator $e^{-i\pi J_z^2}$ in the qubit picture:

$$\begin{aligned} e^{-i\pi J_z^2} &= \exp\Big[-i\frac{\pi}{4}(Z_1+\cdots+Z_n)^2\Big]\\ &= \prod_{\vec{m}}\exp\Big[-i\frac{\pi}{4}\binom{2}{\vec{m}}Z_1^{m_1}\cdots Z_n^{m_n}\Big], \end{aligned} \tag{4}$$

where $\vec{m} = (m_1, \ldots, m_n)$ is a multi-index of positive integers that sums to 2 and $\binom{2}{\vec{m}}$ is a multinomial coefficient. We separate the multi-indices into two types: those containing a single slot i such that $m_i = 2$ and those that do not. The former will happen $n = 2j$ times (one for each qubit) and the associated Pauli operator squares to the identity:

$$\exp\Big[-i\frac{\pi}{4}I\Big]^n\prod_{\vec{m}\neq 2}\exp\Big[-i\frac{\pi}{4}\binom{2}{\vec{m}}Z_1^{m_1}\cdots Z_n^{m_n}\Big]. \tag{5}$$

The remaining multi-indices each have exactly two different slots equal to 1 and so the multinomial coefficient is always 2. The exponential consequently reduces to

$$\begin{aligned} e^{-i\frac{n\pi}{4}}\prod_{\vec{m}\neq 2}\Big(I^{\otimes n}\cos\frac{\pi}{2} - iZ_1^{m_1}\cdots Z_n^{m_n}\sin\frac{\pi}{2}\Big)\\ = e^{-i\frac{n\pi}{4}}\prod_{\vec{m}\neq 2}\big(-iZ_1^{m_1}\cdots Z_n^{m_n}\big). \end{aligned} \tag{6}$$

It is already clear from Eq. (6) that $e^{-i\pi J_z^2}$ is a local unitary and so does not affect any correlations between the qubits. Hence the entanglement generated between the qubits is periodic in the chaoticity parameter with period $\Delta\kappa = 2\pi j$ [18].

Equation (6) can be written in a more compact form as $e^{-i\pi J_z^2} = (-1)^{j^2}Z_1^{n-1}\cdots Z_n^{n-1}$, which is clearly symmetric. This breaks into two cases:

$$e^{-i\pi J_z^2} = \begin{cases}(-1)^j Z^{\otimes n} & \text{integer},\\ e^{-i\frac{\pi}{4}}I^{\otimes n} & \text{half-integer}.\end{cases} \tag{7}$$

Now we derive our main result: the existence of temporal periodicities for three special values of twist strength,

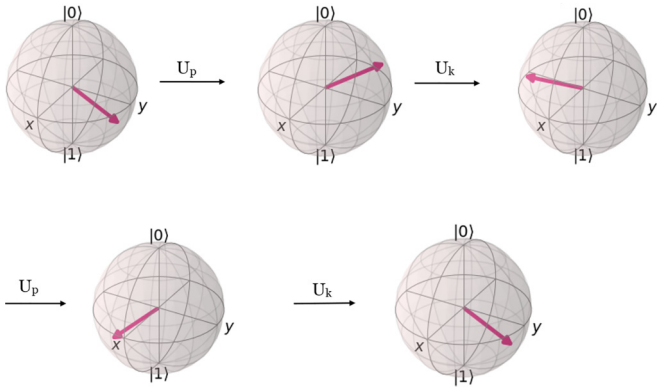

FIG. 2. Evolution of the Bloch vector of any reduced qubit state for $\kappa = 2\pi j$. After two kicks the state returns to its initial point, showing a two-step temporal periodicity. The initial point is $(\theta, \phi) = (2.25, 2.0)$.

$\{2\pi j, \pi j, \frac{\pi j}{2}\}$, each of which are split into cases of integer and half-integer spins.

A. Twist strength $\kappa = 2\pi j$

The twist part of the Floquet operator in the case of $\kappa = 2\pi j$ is given by Eq. (7). Like many of the results here, the consequences on temporal periodicity strongly depend on whether the spin is integer or half-integer. In the case of integer spin the evolution squares to the identity regardless of the y-rotation angle. This can be seen using the integer form of Eq. (7) and writing the y rotation in the qubit picture as $e^{-ipJ_y} = (I\cos\frac{p}{2} - iY\sin\frac{p}{2})^{\otimes n}$. And because in this case $U_{2\pi j}^2$ is simply a composition of symmetric local unitaries, it suffices to consider a single tensor factor:

$$\left[Z\left(I\cos\frac{p}{2} - iY\sin\frac{p}{2}\right)\right]^2 = I\left(\cos^2\frac{p}{2} + \sin^2\frac{p}{2}\right) - \frac{1}{2}(ZX + XZ)\sin p = I, \tag{8}$$

with the last line coming from the anticommutation relations of Pauli matrices. Figure 2 shows this two-step evolution of each qubit on the Bloch sphere. After the first y rotation the twist effectively acts as a π rotation about the z axis. Consequently, the second y rotation then undoes the first and the second twist rotates back to the starting point. Note that this demonstration depends on each step being a symmetric local unitary, meaning that a spin coherent state will remain so throughout and no correlations are ever generated.

In the case of half-integer spin the twist becomes a scaled identity operator (7), leading possibly to a p-dependent temporal periodicity (up to an irrelevant global phase): $U_{2\pi j}^N = I$ if $N = \frac{2\pi}{p} \in \mathbb{N}$. Hence only when p is a rational fraction of π does there exist a temporal periodicity at this twist strength. It is interesting that in the half-integer case the rotation angle p is critical for determining the existence of a temporal periodicity, while in the integer case p has no effect.

B. Twist strength $\kappa = \pi j$

This twist strength yields a more interesting temporal periodicity that also depends on the spin being integer or half-integer; details can be found in Appendix B.

Following a similar argument from earlier, the general expression for the twist unitary $e^{-i\frac{\kappa}{2j}J_z^2}$ is

$$e^{-i\frac{\kappa}{8j}n}\prod_{\vec{m}\neq 2}\left(I^{\otimes n}\cos\frac{\kappa}{4j} - iZ_1^{m_1}\cdots Z_n^{m_n}\sin\frac{\kappa}{4j}\right), \tag{9}$$

which reduces to

$$e^{-i\frac{\pi}{2}J_z^2} = e^{-i\frac{\pi}{8}n}\prod_{\vec{m}\neq 2}\frac{1}{\sqrt{2}}\left(I^{\otimes n} - iZ_1^{m_1}\cdots Z_n^{m_n}\right) \tag{10}$$

when $\kappa = \pi j$. This appears to be a difficult expression to evaluate but simplifies, for integer spins, to

$$e^{-i\frac{\pi}{2}J_z^2} = e^{-i\frac{\pi}{4}}\frac{I^{\otimes n} + i(iZ)^{\otimes n}}{\sqrt{2}}, \tag{11}$$

as can be verified by comparing the two actions on the computational basis in $(\mathbb{C}^2)^{\otimes 2j}$. This can also be found using the Gaussian sum decomposition result from [17]. Now, writing the y rotation in the qubit picture, we find that the Floquet operator exhibits the finite-time periodicity

$$U_{\pi j}^8 = I \quad \forall \text{ integer } j. \tag{12}$$

This can be shown by establishing that $U_{\pi j}^4$ reduces to

$$\left[\frac{e^{-i\frac{\pi}{4}}}{\sqrt{2}}(I^{\otimes n} + i(iZ)^{\otimes n})\left(\frac{I - i\sigma_y}{\sqrt{2}}\right)^{\otimes n}\right]^4 = -(iY)^{\otimes n} \tag{13}$$

through repeated use of the Pauli group commutation relations. As n is currently an even integer and $Y^2 = I$, this is enough to give Eq. (12). The same calculation may be repeated for $\kappa = \pi j + 2\pi j = 3\pi j$, which also shows the period 8 periodicity. While expected from the $2\pi j$ periodicity in κ established above and in [18], this additional calculation is necessary to conclude the stronger notion of temporal periodicity of the state itself rather than just the correlations. For example, any SU(2) rotation with an angle incommensurate to π will produce a sequence of spin coherent states—and therefore a period-1 recurrence in any qubit correlations—that nevertheless does not return to the original state exactly.

In contrast to the previous twist strength of $\kappa = 2\pi j$, here entanglement is generated (and destroyed) throughout the period-8 orbit. This can be seen from Eq. (11), which is clearly not a symmetric local unitary. Figure 3 shows the orbit of a spin coherent state initially centered at $(\theta = 2.25, \phi = 2.0)$. After the initial rotation about the y axis, we see the action of (11) "splitting" the state into a catlike superposition. A second kick iteratively produces a balanced superposition of four spin coherent states. Another two kicks recombine this state into the initial spin coherent state but reflected about the y axis (13). Another four kicks repeats this process, resulting in a recurrence of the initial state. This periodic behavior appears to have no analog in the classical kicked top (not least of which at $\kappa = \pi j$) and so represents a departure from the classical-quantum correspondence for all j.

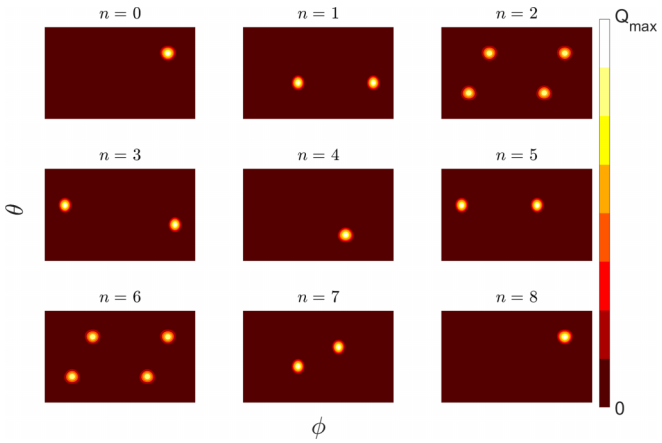

FIG. 3. Husimi function evolution at $\kappa = \pi j$ of a spin coherent state starting at $(\theta, \phi) = (2.25, 2.0)$ over eight kicks at $j = 50$. The state splits and becomes entangled, then recombines back to the original unentangled position. $Q_{\max}$ corresponds to the maximum height of the Husimi distribution in each plot.

It should also be noted that while the above is the generic temporal periodicity, certain states related to the Hamiltonian symmetries will experience a shorter orbit. In particular, if we take the initial state as $|+\rangle_y$, i.e., $(\theta, \phi) = (\pi/2, \pi/2)$, then the rotation part of the unitary will be ineffective. The twist (11) will create the superposition of $|+\rangle_y$ and $|-\rangle_y$; it can be shown that the evolution reduces to a period-4 orbit for even integer spins and a period-2 orbit for odd integer spins. See also [15] for a related analysis.

In the case of half-integer spin and $\kappa = j\pi$ the twist operator becomes

$$e^{-i\frac{\pi}{8}J_z^2} = \frac{e^{-i\frac{\pi}{8}}}{\sqrt{2}}\left[\left(\frac{I + iZ}{\sqrt{2}}\right)^{\otimes n} + \left(\frac{I - iZ}{\sqrt{2}}\right)^{\otimes n}\right] \tag{14}$$

in the qubit picture. Similar to the integer case, repeated and iterated use of the Pauli group commutation relations shows that Eq. (14) raised to the sixth power yields a π rotation up to phase

$$U_{\pi j}^6 = e^{-i\frac{3\pi}{4}}(iY)^{\otimes n}. \tag{15}$$

The recurrence then occurs after 12 kicks:

$$U_{\pi j}^{12} = e^{-i\frac{\pi}{2}}I \quad \forall \text{ half-integer } j, \tag{16}$$

which is a finite temporal periodicity up to the global phase. This recurrence was first discovered for the spin-$\frac{3}{2}$ case in [16]; here we have shown it exists in all dimensions. As expected, a similar calculation shows another period-12 recurrence at $\kappa = \pi j + 2\pi j = 3\pi j$.

Again starting with a generic spin coherent state (i.e., a symmetric product state in the qubit picture), entanglement is generated and destroyed throughout its 12-step orbit. Similar to Fig. 3, the generation occurs during the recursive splitting of the state into a successive catlike superposition and the destruction occurs during the subsequent recombination thereof. States associated with Hamiltonian symmetries again experience a reduced orbit length. For the initial state as $|+\rangle_y$, i.e., $(\theta, \phi) = (\pi/2, \pi/2)$, the evolution reduces to a period-3 orbit.

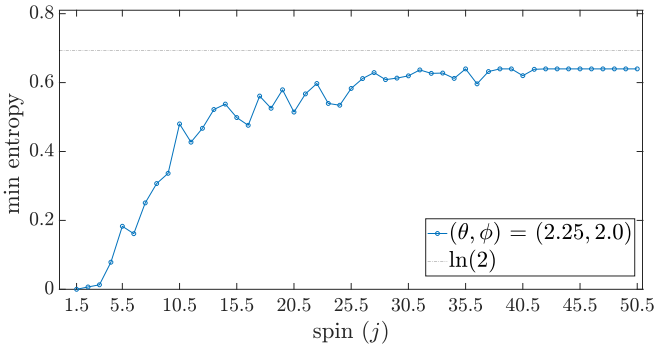

FIG. 4. Minimum single-qubit entropy within the first 5000 kicks at $\kappa = \frac{\pi j}{2}$ as a function of spin. Initial spin coherent state is centered at $(\theta, \phi) = (2.25, 2.0)$.

C. Twist strength $\kappa = \frac{\pi j}{2}$

This twist strength has the most apparent difference between integer and half-integer spin. In the integer case, numerical calculations indicate a period-48 recurrence,

$$U_{\frac{\pi j}{2}}^{48} = I \quad \forall \text{ integer } j. \tag{17}$$

This has been confirmed up to spin $j = 500$ where the Hilbert–Schmidt distance $\|U_{\frac{\pi j}{2}}^{48} - I\|_2$ remains zero within our working error tolerance of 10^{-10}. And similar to the $\kappa = \pi j$ case (both integer and half-integer) here the Floquet operator raised to half the period (i.e., 24) acts as a π rotation about the y axis up to the global phase. Catlike splitting and recombination cycles were furthermore observed in the Husimi representation of a generic spin coherent state (see Appendix A and Ref. [19] for Husimi function details). Numerics also confirm a period-48 recurrence at $\kappa = \frac{\pi j}{2} + 2\pi j = \frac{5\pi j}{2}$.

We also note what appears to be two higher-frequency recurrences present in low dimensions at this chaoticity value: for $j = 1$ and $j = 3$ the evolution repeats after only 16 kicks rather than 48. This observation is distinct from the continued theme of the special states $|\pm\rangle_y$ experiencing a reduced orbit of 24 for even values of j and 4 for odd values of j, which we numerically verified.

In the half-integer case we surprisingly find no temporal periodicity for $\kappa = \frac{\pi j}{2}$. This was numerically concluded by computing the entanglement entropy of any one of the reduced constituent qubits,

$$\rho = \frac{1}{2}\begin{pmatrix} 1 - \langle S_z\rangle & \langle S_-\rangle \\ \langle S_+\rangle & 1 + \langle S_z\rangle \end{pmatrix}, \tag{18}$$

via the collective spin observables $\{S_z, S_\pm = S_x \pm iS_y\}$, where $S_i = J_i/j$ [20]. All that is needed to conclude the lack of a global recurrence is the identification of a spin coherent state that never returns to product form. We thus focus on our running example of $|\theta, \phi\rangle = |2.25, 2.0\rangle$ and found that up to spin $j = 50\frac{1}{2}$ the single qubit dynamical entropy never falls below 10^{-5} within the first 5000 kicks. In fact, the entropy generally increased with dimension. Figure 4 plots the smallest entanglement entropy of any qubit throughout the first 5000 kicks. As can be seen, higher spins experience a highly entangled orbit, remaining close to the upper bound of $S_{\max} = \ln 2$. Further evidence supporting the lack of a

TABLE I. Recurrence periods for different κ values of form $\frac{m}{2}\pi j$ and $m \in (1, 8)$. Here $\times$ signifies the nonexistence of periodicity and (*) represents results from numerical simulation. The numbers are specific to $p = \frac{\pi}{2}$ with the exception of the integer-spin period-2 orbit for $\kappa = 2\pi j$, which is independent of p.

Chaos parameter	Period	
m ($\kappa = \frac{m}{2}\pi j$)	Integer spin	Half-integer spin
8	4	4
4	2	4
1, 3, 5, or 7	48*	$\times$*
2 or 6	8	12

recurrence can be found in the specific case of spin $j = \frac{3}{2}$, using the single-qubit linear entropy for the $|+\rangle_y$ state as mentioned in [16]. We found that the linear entropy does not exactly vanish within the first million kicks. The lack of periodicity at this κ value also shows that, in general, not all twist strengths commensurate to π yield an exact recurrence.

D. Summary and other recurrences

Table I summarizes our results. With these recurrences established, a natural question to ask is if there are others. To this end, we have performed a numerical search for such recurrences characterized by $\kappa = \pi j \frac{r}{s}$ for all coprime $1 \leqslant r, s \leqslant 10$, for all integer and half-integer spin, up to 15.5 and have found none. This was done by computing the von Neumann entropy for the initial state given by $|\theta, \phi\rangle = |2.25, 2.0\rangle$, up to 500 kicks, and found that minimum value of the entropy for the different sets of r and s up to $j = 15.5$ never falls below 10^{-7}. Numerical simulations suggests that there are no other sets of r and s that show the temporal periodicity than what we have found. This therefore places constraints on any additional values of κ that yield a state-independent finite periodicity.

IV. RELATION TO KICKED ROTOR

It is interesting to compare our results to the quantum resonance behavior found in the quantum kicked rotor [4,21,22]. This purely quantum dynamics occurs when one of the Hamiltonian parameters takes the form $4\pi \frac{r}{s}$ and is characterized by quadratic growth of the wave function in momentum space. In contrast, the classical kicked rotor at the same parameter value only has linear scaling. The following works have explained this phenomena using a pseudoclassical theory [23,24]. An interesting exception to this quadratic growth behavior is the case of $r/s = 1/2$, which yields a period-2 state-independent orbit. This special case is known as *quantum antiresonance* due to the complete lack of momentum growth [4].

Reference [17] proposed a kicked top version of the quantum resonance condition as $\kappa = 4\pi \frac{r}{s} j$ for coprime integers r and s, where it may be assumed $r/s < 1$ without loss of generality due to the global symmetry $U_\kappa = U_{\kappa+4\pi j}$. This proposal is motivated by the well-known contraction from the quantum kicked top to the quantum kicked rotor [25], effected via the simultaneous scaling

$$\kappa \sim j, \quad p \sim \frac{1}{j} \quad \text{as } j \to \infty. \tag{19}$$

Here the kicked top parameter κ becomes the relevant parameter in the kicked rotor that controls the existence of resonances [26].

The periodicities examined here do not satisfy the $p \sim 1/j$ scaling (19) and therefore are not to be seen as "precontracted" phenomena, at least not in a strict sense. It is thus interesting that despite only having a partial relationship to the resonance behavior found in the kicked rotor we still observe nonstandard dynamics in the kicked top at these special chaoticity values.

The lone case of $\kappa = 2\pi j$ (i.e., $r/s = 1/2$) for integer spin discussed above actually can be seen as being precontracted. This is because the period-2 orbit does not depend on the rotation angle p and so without loss of generality we may set it to scale as $p \sim 1/j$. Thus the peculiar behavior of quantum antiresonance found in the rotor may be seen as originating in the quantum kicked top. Previous works focusing on quantum correlations [18] or the pseudoclassical framework [17] do not fully capture this specialized antiresonance effect: both approaches depend on the rotation angle p and both predict a higher than necessary orbit period [27].

V. CONCLUSION

Previous studies comparing classical and quantum dynamics in the kicked top largely validate the correspondence principle in the semiclassical regime [6,28]. Other works have gone into characterizing chaos in the deep quantum regime [9,10,14,18,29]. Here we have contributed to the discussion by finding various sets of state-independent, finite-time periodicities that have no classical analog and which exist for all finite spins (i.e., both the deep quantum and semiclassical regimes). And since the classical top is always recovered in the classical limit for any fixed value of κ [25], the dynamics identified here thus represent a sort of nonuniformity condition in how the quantum evolution transitions to the classical one. Some of these recurrences had been identified earlier for specific spins [14,16,30] or in a semiclassical context [17], but here we have generalized these results. We have analytically shown the existences of sets of recurrences and numerically introduced others. Our work also explains the behavior of OTOC in the kicked top observed in the previous study [30]. A preliminary search for additional "simple" periodicities indicates that if they exist the recurrence time must be relatively large.

Our analysis resolves a confusion over the general relationship between the rationality of the chaoticity parameter κ and the existence of a recurrence in the quantum kicked top. Reference [14] argued that whenever this value is a rational multiple of π the evolution will be periodic in the sense that any initial state will only explore a finite subset of Hilbert space. Reference [18], on the other hand, maintained that this is only true for spin-1 systems; i.e., higher dimensional kicked tops do not experience such finite-orbit periodicity regardless of the chaoticity value. Here we have demonstrated the answer lies somewhere in between. In particular, while recurrences

do exist in all dimensions, and these recurrences do come from a rational κ value, not all rational κ values may yield a recurrence.

We further established a relationship to the quantum resonance phenomenon of the quantum kicked rotor [4] and showed that the peculiar antiresonance effect (i.e., $U^2 = I$) in the kicked rotor may have its origins in the quantum kicked top. Given the link to the kicked rotor and the simple, general criterion for periodicity, it would seem reasonable to expect such nonclassical resonances to occur in other periodic or kicked systems as well. Future work in this direction would help shed light on the complicated route to classical dynamics in chaotic systems.

ACKNOWLEDGMENTS

This work was supported in part by the Natural Sciences and Engineering Research Council of Canada (NSERC). We acknowledge fruitful discussions with A. Jamison and S. Nahar. Wilfrid Laurier University and the University of Waterloo are located in the traditional territory of the Neutral, Anishnawbe, and Haudenosaunee peoples.

APPENDIX A: HUSIMI FUNCTION

To study the quantum-classical correspondence in the quantum kicked top, the Husimi function is often used as an aid to compare quantum vs classical dynamics [6,19]. It is a non-negative quasiprobability distribution defined as

$$Q_\rho(\theta,\phi) := \langle\theta,\phi|\rho|\theta,\phi\rangle, \tag{A1}$$

subject to the normalization condition

$$\frac{2j+1}{4\pi}\int_{S^2} Q_\rho(\theta,\phi)\sin\theta\, d\theta\, d\phi = 1, \tag{A2}$$

where $|\theta,\phi\rangle$ is the standard spin coherent state associated with SU(2) dynamical symmetry [31].

APPENDIX B: MULTIQUBIT EXPRESSIONS

Here we will present the proofs of

$$e^{-i\frac{\pi}{2}J_z^2} = e^{-i\frac{\pi}{4}}\frac{I^{\otimes n} + i(iZ)^{\otimes n}}{\sqrt{2}} \tag{B1}$$

and

$$e^{-i\frac{\pi}{2}J_z^2} = \frac{e^{-i\frac{\pi}{8}}}{\sqrt{2}}\left[\left(\frac{I+iZ}{\sqrt{2}}\right)^{\otimes n} + \left(\frac{I-iZ}{\sqrt{2}}\right)^{\otimes n}\right] \tag{B2}$$

together with their temporal periodicities,

$$U_{\pi j}^8 = I \quad \forall \text{ integer } j \tag{B3}$$

and

$$U_{\pi j}^{12} = e^{-i\frac{\pi}{2}}I \quad \forall \text{ half-integer } j. \tag{B4}$$

This is first done by comparing how the left-hand side (LHS) and right-hand side (RHS) acts on the computational basis,

$$e^{-i\frac{\pi}{2}J_z^2}\left|D_n^{(k)}\right\rangle = e^{-i\frac{\pi}{2}\frac{(n-2k)^2}{4}}\left|D_n^{(k)}\right\rangle, \tag{B5}$$

where

$$\left|D_n^{(k)}\right\rangle = |\underbrace{0\cdots0}_{n-k}\otimes\underbrace{1\cdots1}_{k}\rangle. \tag{B6}$$

Note that any computational basis state with Hamming weight k is an eigenstate of J_z with eigenvalue $\frac{n-2k}{2}$. We now consider integer vs half-integer spin separately.

1. Integer spin

The RHS of Eq. (B2) acting on $|D_n^{(k)}\rangle$ is

$$\begin{aligned} &e^{-i\frac{\pi}{4}}\left[\frac{I^{\otimes n} + i(i\sigma_z)^{\otimes n}}{\sqrt{2}}\right]\left|D_n^{(k)}\right\rangle \\ &\quad= e^{-i\frac{\pi}{4}}\left[\frac{I^{\otimes n} + (i)^{n+1}(-1)^k}{\sqrt{2}}\right]\left|D_n^{(k)}\right\rangle \\ &\quad= e^{-i\frac{\pi}{4}}\left[\frac{1+(i)^{n+1+2k}}{\sqrt{2}}\right]\left|D_n^{(k)}\right\rangle. \end{aligned} \tag{B7}$$

Hence the goal is to show

$$e^{-i\frac{\pi}{2}\frac{(n-2k)^2}{4}} = e^{-i\frac{\pi}{4}}\left[\frac{1+(i)^{n+1+2k}}{\sqrt{2}}\right] \tag{B8}$$

for all k. Here the number of qubits n will be even, $n = 2q$, where $q \in \{1, 2, \ldots, \frac{n}{2}\}$. The LHS of Eq. (B8) reduces to

$$e^{-i\frac{\pi}{2}\frac{(n-2k)^2}{4}} = e^{-i\frac{\pi}{2}(q-k)^2} \tag{B9}$$

$$= \begin{cases} 1 & \text{when } q,k \text{ have the same parity,} \\ -i & \text{when } q,k \text{ have opposite parity,} \end{cases} \tag{B10}$$

while the RHS takes the form

$$e^{-i\frac{\pi}{4}}\left[\frac{1+(i)^{n+1+2k}}{\sqrt{2}}\right] = e^{-i\frac{\pi}{4}}\left[\frac{1+(i)^{2(q+k)+1}}{\sqrt{2}}\right]. \tag{B11}$$

This similarly splits into two forms: $(4l+1)$ when q and k are both even or both odd and $(4l-1)$ otherwise:

$$(i)^{n+1+2k} = \begin{cases} +i & \text{when } 2(q+k)+1 = 4l+1, \\ -i & \text{when } 2(q+k)+1 = 4l-1, \end{cases} \tag{B12}$$

bringing the RHS to

$$\begin{aligned} &e^{-i\frac{\pi}{4}}\left[\frac{1+(i)^{n+1+2k}}{\sqrt{2}}\right] \\ &\quad= \begin{cases} 1 & \text{when } q,k \text{ have the same parity,} \\ -i & \text{when } q,k \text{ have opposite parity.} \end{cases} \end{aligned} \tag{B13}$$

This establishes Eq. (B8) and therefore Eq. (B2).

The temporal periodicity, Eq. (B3), may be shown through repeated use of the Pauli group commutation relations. For any two elements g and h of a group G, the group commutator

is defined as

$$[g, h] := g^{-1}h^{-1}gh. \tag{B14}$$

The rotation component of the Floquet operator in the qubit picture is

$$e^{-ipJ_y} = \left(I\cos\frac{p}{2} - i\sigma_y \sin\frac{p}{2}\right)^{\otimes n}. \tag{B15}$$

For $p = \frac{\pi}{2}$ this reduces to

$$e^{-i\frac{\pi}{2}J_y} = \left(I\cos\frac{\pi}{4} - i\sigma_y \sin\frac{\pi}{4}\right)^{\otimes n} =: \gamma^{\otimes n}. \tag{B16}$$

The group commutation relation between γ and σ_z is computed to be

$$[\sigma_z, \gamma] = \sigma_z^{-1}\gamma^{-1}\sigma_z\gamma = i\sigma_y. \tag{B17}$$

This implies

$$\sigma_z\gamma = -\gamma\sigma_x. \tag{B18}$$

Similarly,

$$\sigma_x\gamma = \gamma\sigma_z. \tag{B19}$$

These relations are then iteratively used to evaluate the fourth power of the full unitary, $U_{\pi j}^4$:

$$\begin{aligned}
&\left[\frac{e^{-i\frac{\pi}{4}}}{\sqrt{2}}\left([I^{\otimes n} + i(i\sigma_z)^{\otimes n}]\gamma^{\otimes n}\right)\right]^4 \\
&= \frac{e^{-i\pi}}{4}[[I^{\otimes n} + i(i\sigma_z)^{\otimes n}]([I^{\otimes n} + i(i\sigma_x)^{\otimes n}]\gamma^{\otimes n})^3]\gamma^{\otimes n} \\
&= \ldots \\
&= \frac{-e^{-i\pi}}{4}[-4(i\sigma_y)^{\otimes n}] \\
&= -(i\sigma_y)^{\otimes n}.
\end{aligned} \tag{B20}$$

Equation (B3) then follows by squaring the above:

$$U_{\pi j}^8 = (-1)^2(-1)^n I^{\otimes n} = I \quad \forall \text{ even } n. \tag{B21}$$

2. Half-integer spin

Equation (B2) and Eq. (B4) follow similarly. Again the twist operator will act in the same way as Eq. (B5). The RHS of Eq. (B2) acts as

$$\begin{aligned}
&e^{-i\frac{\pi}{8}}\frac{1}{\sqrt{2}}[e^{i\frac{\pi}{2}J_z} + e^{-i\frac{\pi}{2}J_z}]\left|D_n^{(k)}\right\rangle \\
&= e^{-i\frac{\pi}{8}}\frac{1}{\sqrt{2}}[e^{i(n-2k)\frac{\pi}{4}} + e^{-i(n-2k)\frac{\pi}{4}}]\left|D_n^{(k)}\right\rangle,
\end{aligned} \tag{B22}$$

meaning we must show

$$e^{-i\frac{\pi}{2}\frac{(n-2k)^2}{4}} = e^{-i\frac{\pi}{8}}\frac{1}{\sqrt{2}}[e^{i(n-2k)\frac{\pi}{4}} + e^{-i(n-2k)\frac{\pi}{4}}] \tag{B23}$$

for all $k \in \{0, \ldots, n\}$. Since n is odd and $2k$ is even, $(n-2k)$ will always be odd and will vary from $-n$ to n.

We define q such that $n - 2k = 2q + 1$, giving

$$e^{-i\frac{\pi}{2}\frac{(n-2k)^2}{4}} = e^{-i\frac{\pi}{2}\frac{(2q+1)^2}{4}} = e^{-i\frac{\pi}{8}}e^{-i\frac{\pi q(q+1)}{2}}. \tag{B24}$$

Here it can be seen that Eq. (B24) cycles through the values $e^{-i\frac{\pi}{8}}\{1, -1, -1, 1\}$ for $q = \{0, 1, 2, 3\}$ mod 4. On the other hand, the RHS of (B23) can be written as

$$\begin{aligned}
&e^{-i\frac{\pi}{8}}\frac{1}{\sqrt{2}}[e^{i(n-2k)\frac{\pi}{4}} + e^{-i(n-2k)\frac{\pi}{4}}] \\
&= e^{-i\frac{\pi}{8}}\frac{1}{\sqrt{2}}\left[2\cos((n-2k)\frac{\pi}{4})\right] \\
&= e^{-i\frac{\pi}{8}}\sqrt{2}\cos\left((2q+1)\frac{\pi}{4}\right).
\end{aligned} \tag{B25}$$

This establishes (B23) and therefore Eq. (14).

This also cycles over $e^{-i\frac{\pi}{8}}\{1, -1, -1, 1\}$ for $q = \{0, 1, 2, 3\}$ mod 4.

To show the half-integer temporal periodicity, Eq. (B4), we again use Eq. (B16) and take the sixth power of the Floquet operator:

$$U_{\pi j}^6 = \left[e^{-i\frac{\pi}{8}}\frac{1}{\sqrt{2}}(e^{i\frac{\pi}{2}J_z} + e^{-i\frac{\pi}{2}J_z})\gamma^{\otimes n}\right]^6. \tag{B26}$$

We use the same technique as in the integer-spin case of commuting the rotation part γ through towards the end using the group commutator relations. This eventually leads to an expression for $U_{\pi j}^6$:

$$\begin{aligned}
&\frac{e^{-i\frac{3\pi}{4}}}{8}[(e^{i\frac{\pi}{2}J_y} + e^{-i\frac{\pi}{2}J_y})(e^{i\frac{\pi}{2}J_z} + e^{-i\frac{\pi}{2}J_z})]^3(\gamma^{\otimes n})^6 \\
&= \frac{e^{-i\frac{3\pi}{4}}}{8}A^3(i\sigma_y)^{\otimes n},
\end{aligned} \tag{B27}$$

where A is composed of the terms inside the square bracket. First we compute A^2:

$$\begin{aligned}
A^2 = {} & (e^{-i\frac{\pi}{2}J_y}e^{-i\frac{\pi}{2}J_z})^2 + 2(e^{+i\frac{\pi}{2}J_y}e^{+i\frac{\pi}{2}J_x}) \\
& + 2(e^{+i\frac{\pi}{2}J_x}e^{+i\frac{\pi}{2}J_z}) + 2(e^{+i\frac{\pi}{2}J_x}e^{-i\frac{\pi}{2}J_z}) \\
& + (e^{+i\frac{\pi}{2}J_y}e^{-i\frac{\pi}{2}J_z})^2 + (e^{-i\frac{\pi}{2}J_y}e^{-i\frac{\pi}{2}J_x}) \\
& + 2(e^{-i\frac{\pi}{2}J_x}e^{-i\frac{\pi}{2}J_z})^2 + (e^{-i\frac{\pi}{2}J_x}e^{+i\frac{\pi}{2}J_z}) \\
& + (e^{-i\frac{\pi}{2}J_y}e^{+i\frac{\pi}{2}J_z})^2 + (e^{-i\frac{\pi}{2}J_y}e^{+i\frac{\pi}{2}J_x}) \\
& + (e^{-i\frac{\pi}{2}J_y}e^{-i\frac{\pi}{2}J_x})^2 + (e^{-i\frac{\pi}{2}J_y}e^{-i\frac{\pi}{2}J_z})^2.
\end{aligned} \tag{B28}$$

Upon another application of A this completely reduces to

$$A^3 = 8I, \tag{B29}$$

where the following relations were used:

$$e^{i\frac{\pi}{2}J_b}e^{-i\theta J_a}e^{-i\frac{\pi}{2}J_b} = \epsilon_{abc}e^{-i\theta J_c}, \tag{B30}$$

$$(e^{\pm i\frac{\pi}{2}J_a}\, e^{\pm i\frac{\pi}{2}J_b})^3 = -I, \quad a, b, c \in \{x, y, z\}. \tag{B31}$$

Equation (B26) then becomes

$$U_{\pi j}^6 = e^{-i\frac{3\pi}{4}}(i\sigma_y)^{\otimes n}, \tag{B32}$$

leading to Eq. (B4):

$$U_{\pi j}^{12} = e^{-i\frac{\pi}{2}}I. \tag{B33}$$

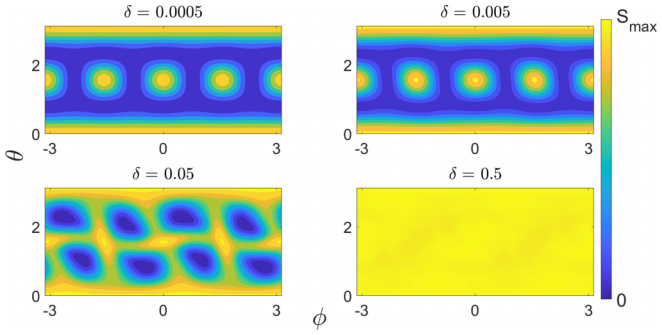

FIG. 5. Average entanglement entropy with $j = 15.5$ and $\kappa = j(\pi + \delta)$, calculated on a grid of 70×140 initial spin coherent states. Each initial state is time averaged over 10 applications of $U^{12}_{j(\pi+\delta)}$ to see the cumulative effect of the error δ. $S_{\max} \in \{2.8 \times 10^{-7}, 1.4 \times 10^{-3}, 0.5574, 0.6863\}$ is the maximum entropy achieved for $\delta \in \{5 \times 10^{-4}, 5 \times 10^{-3}, 0.05, 0.5\}$, respectively.

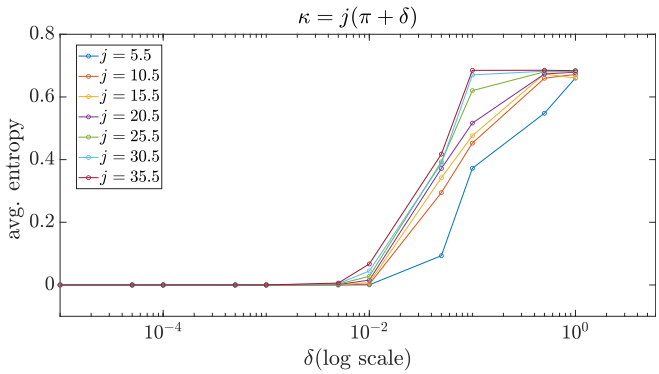

FIG. 6. Mean value of time average entanglement entropy for different spin (j) and $\kappa = j(\pi + \delta)$, calculated on a grid of 70×140 initial spin coherent states. Each initial state is time averaged over 10 applications of $U^{12}_{j(\pi+\delta)}$.

APPENDIX C: STABILITY

In the main section we showed that for certain values of the chaoticity parameter κ (see Table I of the main section), the quantum kicked top unitary experiences a state-independent temporal periodicity and therefore does not reflect the classical dynamics, chaotic or otherwise. The next natural step is to consider what happens as the twist strength is slightly detuned from the exact recurrence values found above. Here we discuss the stability of these special values $\tilde{\kappa}$ via perturbations of the form $\kappa_\delta = j(\pi + \delta)$, where δ is some small deviation incommensurate to π. The Floquet operator becomes

$$U^N_{\tilde{\kappa}+\delta} = \left[\exp\left(-i\frac{j(\pi+\delta)}{2j} J_z^2 \right) \exp\left(-i\frac{\pi}{2} J_y \right) \right]^N = \left[\exp\left(-i\frac{\delta}{2} J_z^2 \right) \cdot U_{\tilde{\kappa}} \right]^N, \tag{C1}$$

where N is the orbit length of the periodicity at $\tilde{\kappa}$ summarized in Table I of the main section.

We proceed by studying the entanglement entropy S of one of the reduced qubits. As spin coherent states are product states in the qubit picture, when there is no perturbation ($\delta = 0$) the entropy of the state $U^N_{\tilde{\kappa}}|\theta, \phi\rangle$ must vanish. Hence as δ slowly increases so too must the entropy, reflecting the change in dynamics from finite recurrence to standard kicked top evolution. Figure 5 shows the entropy for $j = 15.5$, $\kappa = j(\pi + \delta)$ with different δ values, averaged over the application of $U^N_{\kappa_\delta}$ 10 times. That is,

$$\frac{1}{10} \sum_{n=1}^{10} S\big(U^{12n}_{j(\pi+\delta)}|\theta, \phi\rangle\big). \tag{C2}$$

This coarse-grained evolution and averaging is done to capture the cumulative effect of the perturbation δ on the ability of the orbit to return a spin coherent state after N kicks (where in this example $N = 12$ because the spin is half-integer and $\kappa = \pi j$).

There is a clear change in the average dynamics as the perturbation increases, with the relatively strong value of $\delta = 0.5$ showing an entropy plot that matches the phase space structure of the highly chaotic classical kicked top associated to $\kappa = 15.5\pi$. This gradual change is attributed to the shearing from the intermediate squeezing operator $e^{-i\frac{\delta}{2}J_z^2}$, see Eq. (C1), on each superposed spin coherent state arising from $U_{\tilde{\kappa}}$. This intermediate shearing delocalizes the constituent spin coherent states over phase space, which then inhibits their recombination effect typical of Fig. 2 of the main section.

We have also found that the rate of the transition between periodic dynamics and standard dynamics (i.e., as δ increases) largely depends on both $\tilde{\kappa}$ and j. Figure 6 shows the mean value of the time-averaged entanglement entropy over the entire phase space with 70×140 initial spin coherent states. It can be observed that, for different values of spin j, the system becomes unstable at different values of δ. The relation between δ and instability of these special parameters can be explored in future works.

[1] S. Fortin and O. Lombardi, The correspondence principle and the understanding of decoherence, Found. Phys. **49**, 1372 (2019).

[2] M. C. Gutzwiller, *Chaos in Classical and Quantum Mechanics* (Springer-Verlag, Berlin, 1990).

[3] G. Casati, B. V. Chirikov, F. M. Izraelev, and J. Ford, Stochastic behavior of a quantum pendulum under a periodic perturbation, in *Stochastic Behavior in Classical and Quantum Hamiltonian Systems*, edited by G. Casati and J. Ford (Springer Berlin Heidelberg, Berlin, Heidelberg, 1979), pp. 334–352.

[4] F. M. Izrailev and D. L. Shepelyanskii, Quantum resonance for a rotator in a nonlinear periodic field, Theor. Math. Phys. **43**, 553 (1980).

[5] G. Casati and I. Guarneri, Non-recurrent behaviour in quantum dynamics, Commun. Math. Phys. **95**, 121 (1984).

[6] M. Kumari and S. Ghose, Quantum-classical correspondence in the vicinity of periodic orbits, Phys. Rev. E **97**, 052209 (2018).

[7] F. Haake, M. Kuś, and R. Scharf, Classical and quantum chaos for a kicked top, Z. Phys. B **65**, 381 (1987).

[8] S. Chaudhury, A. Smith, B. E. Anderson, S. Ghose, and P. S. Jessen, Quantum signatures of chaos in a kicked top, Nature (London) **461**, 768 (2009).

[9] C. Neill, P. Roushan, M. Fang, Y. Chen, M. Kolodrubetz, Z. Chen, A. Megrant, R. Barends, B. Campbell, B. Chiaro, A. Dunsworth, E. Jeffrey, J. Kelly, J. Mutus, P. J. J. O'Malley, C. Quintana, D. Sank, A. Vainsencher, J. Wenner, T. C. White, A. Polkovnikov, and J. M. Martinis, Ergodic dynamics and thermalization in an isolated quantum system, Nat. Phys. **12**, 1037 (2016).

[10] V. R. Krithika, V. S. Anjusha, U. T. Bhosale, and T. S. Mahesh, NMR studies of quantum chaos in a two-qubit kicked top, Phys. Rev. E **99**, 032219 (2019).

[11] S. Ghose and B. C. Sanders, Entanglement dynamics in chaotic system, Phys. Rev. A **70**, 062315 (2004).

[12] S. Ghose, R. Stock, P. Jessen, R. Lal, and A. Silberfarb, Chaos, entanglement, and decoherence in the quantum kicked top, Phys. Rev. A **78**, 042318 (2008).

[13] M. Lombardi and A. Matzkin, Entanglement and chaos in the kicked top, Phys. Rev. E **83**, 016207 (2011).

[14] J. B. Ruebeck, J. Lin, and A. K. Pattanayak, Entanglement and its relationship to classical dynamics, Phys. Rev. E **95**, 062222 (2017).

[15] V. Madhok, S. Dogra, and A. Lakshminarayan, Quantum correlations as probes of chaos and ergodicity, Opt. Commun. **420**, 189 (2018).

[16] S. Dogra, V. Madhok, and A. Lakshminarayan, Quantum signatures of chaos, thermalization, and tunneling in the exactly solvable few-body kicked top, Phys. Rev. E **99**, 062217 (2019).

[17] Z. Zou and J. Wang, Pseudoclassical dynamics of the kicked top, Entropy **24**, 1092 (2022).

[18] U. T. Bhosale and M. S. Santhanam, Periodicity of quantum correlations in the quantum kicked top, Phys. Rev. E **98**, 052228 (2018).

[19] G. S. Agarwal, Relation between atomic coherent-state representation, state multipoles, and generalized phase-space distributions, Phys. Rev. A **24**, 2889 (1981).

[20] D. Baguette, T. Bastin, and J. Martin, Multiqubit symmetric states with maximally mixed one-qubit reductions, Phys. Rev. A **90**, 032314 (2014).

[21] S. Fishman, D. R. Grempel, and R. E. Prange, Chaos, quantum recurrences, and anderson localization, Phys. Rev. Lett. **49**, 509 (1982).

[22] J. F. Kanem, S. Maneshi, M. Partlow, M. Spanner, and A. M. Steinberg, Observation of high-order quantum resonances in the kicked rotor, Phys. Rev. Lett. **98**, 083004 (2007).

[23] V. V. Sokolov, O. V. Zhirov, D. Alonso, and G. Casati, Quantum resonances of the kicked rotor and the SU(q) group, Phys. Rev. Lett. **84**, 3566 (2000).

[24] S. Wimberger, I. Guarneri, and S. Fishman, Classical scaling theory of quantum resonances, Phys. Rev. Lett. **92**, 084102 (2004).

[25] F. Haake and D. L. Shepelyansky, The kicked rotator as a limit of the kicked top, Europhys. Lett. **5**, 671 (1988).

[26] Note that despite $j \to \infty$ the above is not to be considered a classical limit as the quantum kicked rotor is a fully quantum object—hence *contraction*. In this contraction one does not regularize the observables to A/j.

[27] Reference [18] predicts a period-2 orbit in the quantum correlations at this chaoticity value. This is not wrong, but, as shown for the case of $\kappa = 2j\pi$, no entanglement is generated in the intermediate state and therefore the quantum correlations actually experience a period-1 orbit, while the state experiences a period-2 orbit.

[28] X. Wang, S. Ghose, B. C. Sanders, and B. Hu, Entanglement as a signature of quantum chaos, Phys. Rev. E **70**, 016217 (2004).

[29] A. Anand, S. Srivastava, S. Gangopadhyay, and S. Ghose, Simulating quantum chaos on a quantum computer, arXiv:2107.09809.

[30] S. PG, V. Madhok, and A. Lakshminarayan, Out-of-time-ordered correlators and the Loschmidt echo in the quantum kicked top: how low can we go? J. Phys. D: Appl. Phys. **54**, 274004 (2021).

[31] F. T. Arecchi, E. Courtens, R. Gilmore, and H. Thomas, Atomic coherent states in quantum optics, Phys. Rev. A **6**, 2211 (1972).